

Molecular Structure Determination by EXAFS of $[Y(NCS)_6]^{3-}$ Units in Solid State and in Solution. A Comparison with Density Functional Theory Calculations

Sofía Díaz-Moreno,[†] José M. Martínez,[‡] Adela Muñoz-Páez,^{*,†} Hideto Sakane,[§] and Iwao Watanabe^{||}

Instituto de Ciencia de Materiales, C.S.I.C-Universidad de Sevilla, c/Americo Vesputio, s/n 41092 Sevilla, Spain, Departamento de Química Física, Universidad de Sevilla, 41012 Sevilla, Spain, Department of Applied Chemistry, Faculty of Engineering, Yamanashi University, 4-3-11 Takeda, Kofu, Yamanashi 400-8511, Japan, and Department of Chemistry, Graduate School of Science, Osaka University, Machikaneyama 1-1, Toyonaka, Osaka 560-0043, Japan

Received: May 5, 1998; In Final Form: July 22, 1998

The structure of one of the rare octahedral Y^{3+} complexes, hexakis(thiocyanato-N)yttrate(III), has been elucidated with extended X-ray absorption fine structure (EXAFS) spectroscopy and confirmed by density functional theory (DFT) calculations. The analysis of EXAFS spectra indicates coordination through nitrogen atoms, already suggested by IR and NMR data, and provides information about the linear arrangement of the NCS^- ligands with the yttrium atoms inside the complex. This arrangement emphasizes multiple scattering contributions to the EXAFS signal, due to the focusing scattering effect, and allows the accurate determination of the structure of the whole complex up to the third coordination shell, which is distant by more than 5 Å from the absorbing atom, Y, a resolution without precedent in the use of the technique. The best reproduction of the solid state and acetonitrile solution spectra was achieved with the same structure: a symmetric octahedron with coordination distances equal to 2.36(1), 3.5(1), and 5.1(2) Å for Y–N, Y–C, and Y–S shells, respectively, the only difference between both spectra being the higher dynamic disorder of the solution spectrum. DFT calculations predict this geometry as the most stable, discarding other arrangements in which the coordinating atom is sulfur. The agreement between EXAFS data and DFT optimized structure is quite high, and differences between predicted and experimental IR bands are below 5%.

Introduction

There is an increasing interest in the study of Y^{3+} complexes because of its applications in homogeneous catalysis. Attention has been focused on the study of organometallic complexes, particularly those involving cyclopentadienyl (Cp) and Cp-type ligands because of their activity in oligomerization reactions.¹ Although the general trends in the structure and reactivity of this element are similar to those of the heavier lanthanides, many basic structural aspects of Y^{3+} coordination compounds remain unknown. This element shows a wide variety of coordination environments, the octahedral geometry appearing in a few stable complexes. But to our knowledge, the detailed structure of octahedral Y^{3+} complexes, among which one of the few well authenticated is that formed with thiocyanate ligands,² has not been reported experimentally or theoretically.

Thiocyanate complexes of the transition metals have attracted the attention of several research groups in the past decades because of its ambidentate character that allows the coordination through the N atom, the S atom, or a bridging mode.³ The different coordination modes produce significant changes in the electronic structure of the anion reflected in the frequencies of the IR active modes⁴ and in the chemical shift of the NMR

spectra signals,⁵ the latter usually applied to dissolved species in liquid solution. In the studies using these techniques, values of a given parameter, NMR chemical shift or IR band position, are presented for a series of thiocyanate complexes in which the central atom, the metal charge or the counterion, are changed, providing in this way relative values and general trends. Direct structural information about this type of compound in solid state has been obtained with XRD.⁶ The recent application of X-ray scattering techniques to the study of liquid solutions provides information about the structure of metal solvates and coordination complexes, although this technique is restricted to medium- or high-concentrated aqueous solutions.⁷ By use of this technique, it has been shown that tetrakis(thiocyanate) complexes were predominantly formed with Zn^{2+} , Cd^{2+} , and Hg^{2+} ions and that thiocyanate ligands coordinate Hg^{2+} ions through S atoms, Zn^{2+} ions through N atoms, and Cd^{2+} through both N and S atoms.⁸

Suitable techniques to investigate the possible structural changes induced by solvent effects or distortions due to packing conditions within the crystal are X-ray absorption fine structure spectroscopies (EXAFS and XANES), which allow the study of the investigated species both in solid state and in solution within a wide range of concentrations, detecting short- and long-range order.⁹ These techniques have been successfully applied by the authors to study the solvation structure of ionic solutions, studying both first- and second-shell coordination complexes.^{10–12} Ozutsumi et al. have used it to solve the local structure around Cd^{2+} cations in the tetrakis(thiocyanate)cadmates dissolved in

* Corresponding author. E-mail: adela@cica.es. Fax: 34-95-4460665.

[†] Instituto de Ciencia de Materiales, C.S.I.C. Universidad de Sevilla.

[‡] Departamento de Química Física, Universidad de Sevilla.

[§] Yamanashi University.

^{||} Osaka University.

dimethyl sulfoxide, detecting coordination of thiocyanate ligands through nitrogen and sulfur atoms. These authors have investigated only the first coordination shell, finding coordination distances of 2.22 and 2.62 Å for Cd–N and Cd–S bonds, respectively.¹³ Since these techniques provide *average* information on the local structure around a given atom, it can be complemented by the information supplied by NMR and IR spectroscopies.

In contrast with the abundant literature that can be found for transition metal thiocyanates, the references concerning lanthanide thiocyanates are very scarce. To our best knowledge, there is only one XRD study of the parent compound [Er(SCN)₆]³⁻ in the solid state¹⁴ and another work including IR data of some lanthanide and actinide complexes.¹⁵

Herewith, we report an EXAFS study of the molecular structure of [Y(SCN)₆]³⁻ species in the solid state, as [Bu₄N]₃[Y(SCN)₆], and in acetonitrile solution. This solvent was chosen because acetonitrile molecules do not enter the first coordination sphere of Y³⁺ ions as water molecules do, and thus, the complex is not disrupted by the solution process. The study includes the three shells of atoms forming the coordinating ligands. Moreover, the ¹H and ¹³C{¹H} NMR spectra of the same species in acetonitrile solution have been recorded to check for the existence of different isomers or distortions inside the complex. The IR spectra of the complex in the solid state has been recorded as well with the same aim. The study is completed with a set of DFT calculations, a methodology that has been successfully applied very recently in the study of three coordinated Cu⁺ thiocyanates¹⁶ to transition metal complexes^{17,18} and to many other organic and inorganic systems.¹⁹

Experimental Section

The complex [Bu₄N]₃[Y(SCN)₆] was deposited from an ethanol solution containing YCl₃ and tetra-*n*-butylammonium-thiocyanate in a molar ratio of 1:10.¹⁴ It is soluble in several organic solvents, such as acetonitrile, and partially decomposes in water by replacement of some SCN⁻ ligands by water molecules.

NMR spectra were recorded on a Bruker DRX 500 MHz spectrometer. ¹³C{¹H} chemical shifts for CH₃- and CH₂- groups in the Bu₄N⁺ cation were 13.95, 20.35, 24.35, and 59.25 ppm, and the shift was 118.2 ppm for CD₃CN. They were referenced to the residual signals of the deuterated solvent and are all reported in ppm downfield from SiMe₄. IR spectra were recorded in the solid state, mixing the sample with KBr, in a Nicolet 510 FT-IR spectrometer.

The EXAFS measurements of the Y–K edge at 17.053 keV were carried out at the Photon Factory of the Institute of Materials Structure Science in Tsukuba (Japan) at beamline 10B. The ring current was 300 mA, and the ring energy was 2.5 GeV. A high-resolution Si(311) channel-cut monochromator was used. Calibration was carried out with a Nd foil. Data were collected in transmission mode using ionization chambers as detectors. At least four scans were recorded for each sample to minimize high- and low-frequency noise by averaging. Liquid samples were recorded in special liquid cells with variable path lengths,²⁰ with path lengths being chosen according to the concentration of the absorbing species. For the 0.2 and 0.5 M solutions the path length was 7 and 5 mm, respectively.

EXAFS Data Analysis. The EXAFS functions $\chi(k)$ were obtained from the X-ray absorption spectra by subtracting a Victoreen curve followed by a cubic spline background removal using the program XDAP²¹ from Utrecht University. Normal-

ization was done by division by the height of the edge. The inner potential, E_0 , was defined as the maximum of the first derivative of the absorption edge. The resulting $\chi(k)$ data were reproduced using the FEFF 6.01 code,²² which performs ab initio calculations of curved wave XAFS spectra, taking into account single and multiple scattering (SS and MS) contributions. Phase shift and backscattering amplitude functions for Y–N, Y–C, and Y–S contributions were calculated using the same program.²³

When the FEFF program was used in the calculation of the *N*-coordinated structure, the many-body amplitude reduction factor (S_0^2) was set equal to 0.9, the metal charge was set equal to zero, and the inner potential correction ΔE_0 was 4.0 eV. Taking into account that the formal charge for Y atoms in the complex is +3, several calculations were made giving positive values to the metal charge. Nevertheless, this parameter showed a strong correlation with inner potential correction, so it was set equal to zero. A total of seven parameters were varied during the calculation procedure: the coordination distances for the three coordination shells (R_1 , R_2 , R_3) and four different values for mean-square displacement, σ^2 , the so-called Debye–Waller (DW) factors. Paths with an intensity higher than 4% of that of the first shell were considered, and the total scattering distance, R_{TOT} , was restricted to be equal to or smaller than 5.2 Å. After these restrictions to the solid-state system were imposed, a total of 25 paths were considered, having between two and six legs (one leg is represented by each arrow in Figure 5).

In the only calculation of the *S*-coordinated complex, the same values for the above-mentioned parameters were used with the exception of atomic coordinates, which were taken from the DFT results. Moreover, since the structure was not linear, a smaller number of paths (15) was considered.

To allow the reproduction of the EXAFS analysis, one FEFF 6.01 input file and two output files (FILES.DAT and PATHS.DAT) used during the analysis of [Y(NCS)₆]³⁻ solid-state spectrum are included as Supporting Information in Tables IS–IIS, respectively.

Computational Details for DFT Calculations. Computations, carried out with Gaussian 94 package,²⁴ were performed using the LAN2DZ basis set (Dunning–Huzinaga full double- ζ D95 on carbon and nitrogen atoms²⁵ and Los Alamos effective core potentials and double- ζ basis set on yttrium and sulfur atoms²⁶) together with the hybrid exchange–correlation Becke 3 Lee–Yang–Parr functional²⁷ (B3LYP). Geometries were fully optimized, and the stationary points on the potential energy hypersurface were characterized by harmonic frequency analysis.

Results and Discussion

NMR Spectra. All the signals in the ¹H NMR spectra of [Bu₄N]₃[Y(SCN)₆] in CD₃CN solution show the expected intensities and splitting for one single type of compound. ¹³C{¹H} chemical shifts of coordinated thiocyanate ligands have been shown to be an excellent diagnostic tool for bonding-mode determination of this group.^{5a} Thus, the ¹³C{¹H} spectrum shows a well-resolved sharp peak at 135.1 ppm due to SCN⁻ groups, in addition to the four signals attributable to the Bu₄N⁺ species. According to the results of previous NMR studies of transition metal isothiocyanates, this value is characteristic of octahedral thiocyanate complexes coordinating through the N atom^{5a} and, since it is not split or distorted, it indicates the existence of a single type of isomer.

IR Spectra. Although none of the IR bands of the thiocyanate complex correspond to pure vibration modes, in a good

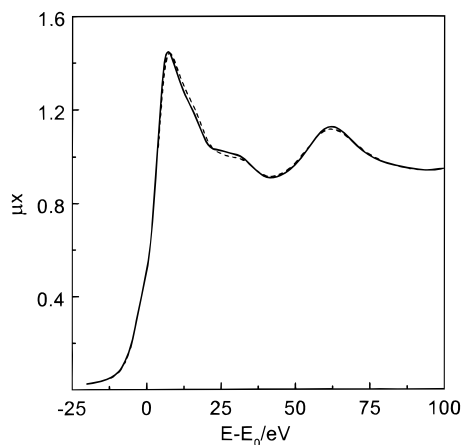


Figure 1. Normalized XANES spectra of Y-K edge absorption spectra of the complex $[\text{Bu}_4\text{N}]_3[\text{Y}(\text{NCS})_6]$ in solid state (solid line) and in 0.5 *m* acetonitrile solution (dashed line).

approximation, the strong, nonsplit band appearing at 2056 cm^{-1} can be attributed to the $\nu(\text{C}\equiv\text{N})$ stretching frequency.⁴ No values have been reported for Y^{3+} thiocyanate complexes, but a value of 2053 cm^{-1} has been reported for the Yb^{3+} octahedral isothiocyanate complex¹⁵ and a value of 2050 cm^{-1} for the corresponding Co^{2+} complex.²⁸ In general, bands appearing within $2130\text{--}2160\text{ cm}^{-1}$ correspond to S-bonded thiocyanate ligands, and bands appearing below this range to N-bonding.¹⁵ A medium-intensity band appearing at 484 cm^{-1} can be attributed to the $\delta(\text{N-C-S})$ bending mode with the first overtone corresponding to the very weak band at 960 cm^{-1} . This bending mode appears at around 420 cm^{-1} for S-bonded thiocyanate complexes and at around 475 cm^{-1} for N-bonded. The positions of all the IR bands related to the SCN^- ligands are compatible with the model proposed by Brown and Knox,^{4b} in which for an N-bonded thiocyanate complex, the formation of the metal-ligand bonds results in a decrease in the $\text{C}\equiv\text{N}$ bond order and in an increase in the C-S bond order from those observed in the free thiocyanate ion.

XANES and EXAFS. Although IR and NMR data are compatible with N-coordination of thiocyanate ligands, these techniques do not provide unambiguous information about the type of coordination. For this reason the X-ray absorption spectra of $[\text{Bu}_4\text{N}]_3[\text{Y}(\text{SCN})_6]$ in the solid state and in 0.5 and 0.2 *m* acetonitrile solution have been recorded. Figure 1 includes the X-ray absorption near-edge spectra (XANES) region of the spectra for the indicated systems. A very similar spectrum was recorded in the 0.2 *m* solution, thus indicating that for moderate concentrations, changes in concentration did not produce detectable structural changes. The solid and 0.5 *m* solution spectra included in the figure appear the same. Since this region of the spectrum is very sensitive to the coordination polyhedra around the absorbing atom,²⁹ this is a clear indication that the coordination environment around Y^{3+} remains basically unchanged after the solution process.

The signal-to-noise ratio is very good up to $k = 12.5\text{ \AA}^{-1}$ in the corresponding EXAFS spectra included in Figure 2a. The solid and solution spectra look very similar, although the solution spectra has a smaller amplitude.

The corresponding Fourier transforms, containing pseudo-radial-distribution functions and plotted in Figure 2b, show three well-resolved intense peaks at 2.4, 3.5, and 5.0 \AA , approximately corresponding to the three coordination shells attributable to the three atoms of the thiocyanate ligands. The only difference between the solid and solution spectra is the smaller amplitude of the peaks at 3.5 and 5.0 \AA in the solution spectra.

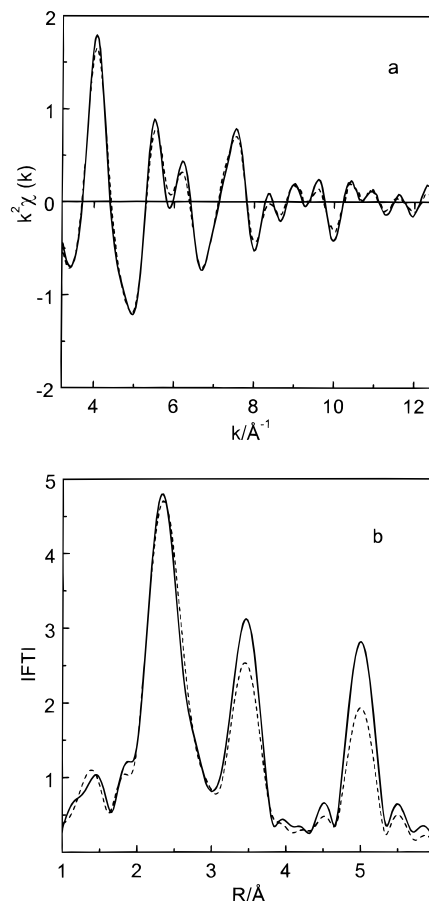


Figure 2. (a) Raw EXAFS signal, k^2 -weighted, of Y-K edge absorption spectra of the complex $[\text{Bu}_4\text{N}]_3[\text{Y}(\text{NCS})_6]$ in solid state (solid line) and in 0.5 *m* acetonitrile solution (dashed line). (b) Magnitude of the Y-N phase-corrected Fourier transform of the EXAFS spectra of Figure 2a, k^3 -weighted; $\Delta k = 3.7\text{--}12.5\text{ \AA}^{-1}$.

In principle, in the solid and solution spectra, the amplitude of both peaks should be negligible compared to that of the first peak because they correspond to shells appearing at longer distances with the same coordination number and similar scattering amplitude. The reason for the high amplitude they show is the “focusing” effect, observed when the absorbing and two or more of the neighbor atoms are arranged in a linear fashion. This arrangement emphasizes multiple scattering contributions to the EXAFS signal.^{9,30} This effect is thus an indication of the linear or quasi-linear arrangement of the ligands with the yttrium atoms within the complex, a piece of information of particular interest, since there is no direct way of obtaining it from IR or NMR spectra. For this reason this arrangement has been a matter of controversy. Moreover, it allows the detection of shells formed by light elements at a distance of more than 4 \AA from the absorbing atom but determines the data analysis strategies. In fact, in most EXAFS analyses it used to be assumed that single scattering (SS) paths had a much greater amplitude than multiple scattering (MS) ones, which were thought to mostly cancel each other.⁹ However, the attempts carried out to reproduce the experimental spectrum of $[\text{Y}(\text{SCN})_6]^{3-}$ using the single scattering approximation failed completely. Not only meaningless values of coordination numbers and mean-square displacements, σ^2 , were obtained but even accurate values of coordination distances could not be obtained. In fact, a shortening of 0.15–0.20 \AA with respect to the expected values in the coordination distances of the higher shells was observed.

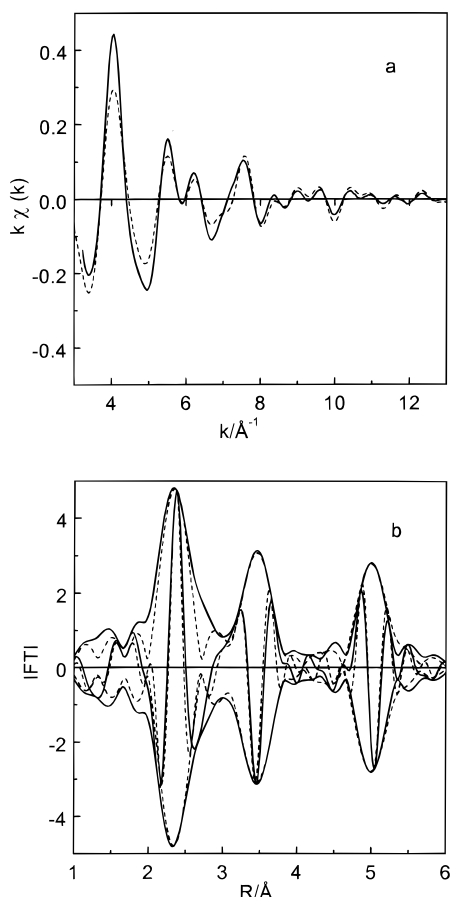


Figure 3. (a) EXAFS spectra, k^2 -weighted, of the complex $[\text{Bu}_4\text{N}]_3\text{[Y(NCS)}_6\text{]}$ in solid state: experimental function (solid line); calculated function with the parameters included in the text (dashed line). (b) Magnitude and imaginary part of the Y–N phase-corrected Fourier transform of the EXAFS spectra in Figure 3a, k^3 -weighted; $\Delta k = 3.7\text{--}12.5 \text{ \AA}^{-1}$.

Various strategies for adding MS to the analysis of the EXAFS functions have been implemented and are already included in packages such as EXCURVE,³¹ GNEXAFS,³² and FEFF.²³ Taking into account the IR and NMR results discussed above, octahedral geometry with coordination through the nitrogen atom was assumed to calculate the EXAFS spectrum plotted in Figure 3a, which includes as well the corresponding experimental spectrum of the solid-state complex. The absolute and imaginary parts of the Y–N phase-corrected Fourier transform appears in Figure 3b. The agreement between experimental and calculated spectra is very good both in k and R spaces.

An additional calculation was carried out for the S-coordinated complex using the structural parameters obtained by DFT calculations (see following section) and the Debye–Waller factors used in the calculation of the N-coordinated complex. Figure 4 shows the magnitude of the FT of the calculated EXAFS spectrum as well as the corresponding FT of the experimental solid-state spectrum. As seen in this plot, neither the amplitude nor the position of the first peak resembles those of the experimental spectrum. Thus, although N and S atoms have similar backscattering power and thus are rather similar elements from an X-ray absorption point of view, the EXAFS technique is capable of distinguishing N- from S-coordination. The additional two peaks appearing in the experimental EXAFS spectrum are completely missing in the calculated one. In fact, they have a very small amplitude. The reason is that in the S-coordinated complex they have a negligible amplitude because

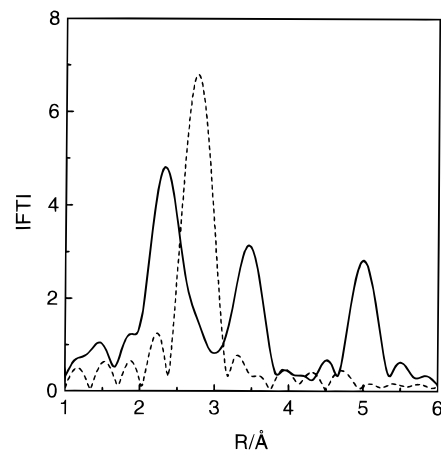


Figure 4. Magnitude of the Y–N phase-corrected Fourier transform of the experimental EXAFS spectra k^3 -weighted, $\Delta k = 3.7\text{--}12.5 \text{ \AA}^{-1}$, of $[\text{Bu}_4\text{N}]_3\text{[Y(NCS)}_6\text{]}$ in solid state (solid line) and of the EXAFS spectra calculated with the atomic coordinates of structure 2 (see Table 1).

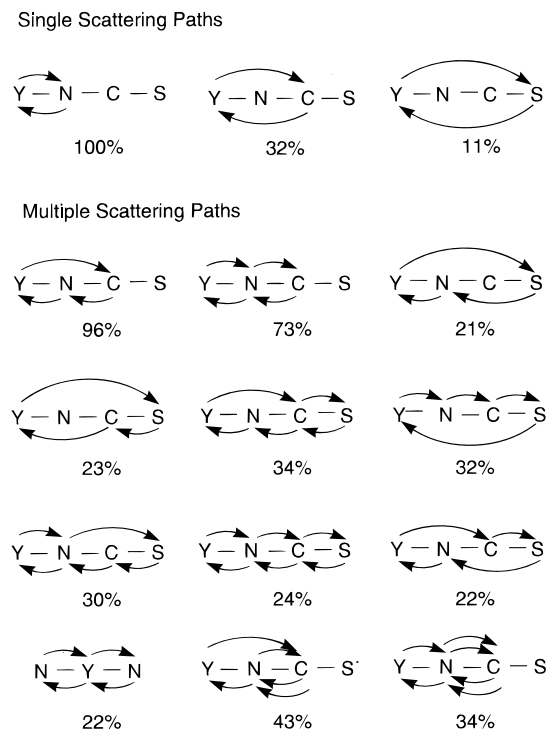


Figure 5. Scattering paths yielding the most intense contributions to the EXAFS spectrum of the complex $[\text{Bu}_4\text{N}]_3\text{[Y(NCS)}_6\text{]}$ in solid state. The number and type of legs are indicated, as well as the amplitudes compared to that of the first shell for zero Debye–Waller factors.

they do not show focusing effects in this nonaligned system. Thus, this structure is fully discarded.

Figure 5 includes a scheme of the SS paths, three in total, and the most intense MS paths used in the calculation of the N-coordinated complex, corresponding to the spectra plotted in Figure 3, showing their respective intensities for zero mean-square displacements ($\sigma^2 = 0$). Among the MS paths included in the figure, the first four correspond to the classical focusing effect, described in several studies^{9,30,33,34} although not fully analyzed in most of them, due to the forward scattering of two neighbors atoms aligned with the absorbing one. Other paths (5) showing a high amplitude (21–36%) are those corresponding to the forward scattering processes involving three scatterer atoms aligned with the absorbing one. This arrangement is not as frequent as the previous one, neither in solid compounds nor

in dissolved molecular species, and its quantitative analysis is rather complicated, since if there is no additional structural information, it requires a very high number of structural parameters to fully optimize it. To our knowledge, there is only one published work where the four-body full multiple scattering analysis has been carried out in cyanide-bridged ion-copper molecular assemblies combining the information obtained from Fe-K and Cu-K edges.³⁵ In this study it has been shown that it is possible to differentiate a linear and a bent four-body geometry in the outer range of the Fourier transform. Moreover, other authors have detected this effect in other solid compounds, calling it "superfocusing" effect,³⁰ but they have not carried out the full MS analysis.

Although it has a smaller amplitude, the contribution from the first coordination shell involving N-Y-N chains is significant as well, with 22% amplitude. It is similar to that found in aquocomplexes,³⁶ where it has an additional contribution from the second hydration shell.^{10,11} Among the 22 MS paths considered, only four included nonaligned atoms, but they had amplitudes smaller than 8% of that of the first shell.

The best reproduction of the spectrum, both in k and R spaces, was obtained for coordination distances of 2.36(1), 3.5(1), and 5.1(2) Å for Y-N, Y-C, and Y-S shells, respectively. Four different values of the Debye-Waller factors, σ^2 , were used for the 25 paths. A value of 0.0030 Å² was used for the first path, corresponding to the SS contribution from the first shell. A value of 0.0053 Å² was used for the next four paths, including SS from the second coordination shell and three more MS contributions. A value of 0.0057 Å² was used for the following 6 and 0.0064 Å² for the remaining 14. (For additional details see Table IIS in Supporting Information). As expected, the higher accuracy was obtained for the first coordination shell, which yielded the most intense contribution to the EXAFS spectrum.

The disagreement between experimental and calculated spectra observed in Figure 3a, particularly around 7 Å⁻¹, can be probably ascribed to the double excitations 1s3d → 5p4d, as observed by the authors in YBr₃ aqueous solutions and by D'Angelo et al. in systems containing Rb.³⁷ The complexity of the spectrum here studied hampered the calculation of this double excitation processes, but the shoulder appearing at around 7.2 Å⁻¹ both in the solid and in the solution spectra and not reproduced in any of the calculated spectra is very similar to that found in the spectra of YBr₃ aqueous solutions.

The obtained parameters are consistent with the values found with XRD for the structure of the parent compound $[\text{Er}(\text{SCN})_6]^{3-}$, for which bond distances are Er-N = 2.34 Å, N-C = 1.10 Å, and C-S = 1.61 Å in a quasi-linear distribution (Er-N-C = 174°, N-C-S = 176°).¹⁴ To our best knowledge, no similar information is available for $[\text{Y}(\text{SCN})_6]^{3-}$ in the solid state or in solution, although its synthesis and chemical analysis have been reported.¹⁴

The best reproduction of the spectrum in acetonitrile solution was obtained for the same structure but with larger values of the Debye-Waller factors, $\sigma^2 = 0.0031$ Å² (1 path), 0.0065 Å² (4 paths), 0.0085 Å² (6 paths), and 0.0090 Å² (14 paths), which causes the decrease in amplitude observed in Figure 2b for the outer shells of the solution spectra. Since the value of the DW factor for the first coordination shell is the same for the solution and for the solid systems, it can be deduced that the Y-N bond strength has not changed substantially after the solution process. On the other hand, since no significant changes within the NCS⁻ ligands are expected between the solid and solution systems, the higher values of DW factors for the second and third

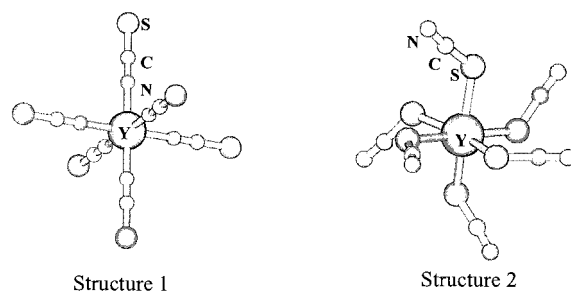


Figure 6. Theoretically optimized structures of N- and S-coordinated complexes.

TABLE 1: Comparison between Theoretical and Experimental Geometrical Parameters

	structure 1	structure 2	EXAFS
Bond Distances (Å)			
$d(\text{Y}-\text{N})$	2.367	4.998	2.36
$d(\text{Y}-\text{C})$	3.565	3.960	3.5
$d(\text{Y}-\text{S})$	5.255	2.841	5.1
Bond Angles (deg)			
$\angle \text{YXC}^a$	180.0	118.0	180.0
$\angle \text{SCN}$	180.0	174.4	180.0

^a X represents the coordinating atom.

coordination shells observed in the solution system should be related with the increased fluctuation of the $\angle \text{YNC}$ angle due to wagging motion of the ligands, which are not as restrained as in the case of the solid system.

Theoretical Calculations. To complete the experimental information already shown, we present in this section theoretical calculations performed using density functional theory.³⁸ Two different arrangements were considered for the interaction between Y^{3+} cation and SCN^- ligands. The first one corresponds to structure 1, where the yttrium atom is coordinated through the nitrogen atom, and the second to structure 2, where the coordinating atom is sulfur. Optimized geometries are shown in Figure 6, and the geometrical parameters can be found in Table 1, where a comparison with previous EXAFS results is done.

The symmetry of structure 1, the N-coordinated complex, is O_h , whereas in structure 2, the S-coordinating complex, this high symmetry is completely lost and is lowered to C_1 . In this sense, it can be observed how in the first structure there is a collinear arrangement between the ligand and the central atom, while in the second situation, values smaller than 180° for the $\angle \text{YSC}$ angle are obtained, on average 118.0°. The internal geometries of SCN^- fragments show differences between the two compounds as well. Thus, the SCN^- fragment is linear in the N-coordinated structure, whereas in the second situation it takes a value of ca. 174.5°. All these geometrical features have been recently observed in detailed theoretical studies of Cu^+ ¹⁶ and Re^{4+} ³⁹ thiocyanates in which bending for the C-S-M and S-C-N angles were observed in the case of the S-bonded isomers.

From a structural point of view the agreement between the parameters calculated for structure 1 and those obtained from the analysis of the EXAFS data is quite reasonable. The largest differences are found for the Y-S distance, which can be due, at least partially, to the internal definition of the SCN^- fragment at the level of theory applied for this study. An optimization of this ligand with a larger basis set,⁴⁰ 3-21+G*, shortens the S-C distance by about 0.07 Å, when compared with the LANL2DZ optimized value (the C-N distance is only 0.01 Å shorter). Structure 1 is about 115 kcal/mol more stable than

structure **2**, so the N-coordinating complex is highly preferred, thus confirming the HSAB principle, since trivalent yttrium cations are typical hard acids, while N atoms are typical hard bases.

Finally, vibrational spectra for the two optimized geometries have been computed. The high symmetry of the N-bonded complex reduces considerably the number of IR active bands in comparison with the structure in which the Y is coordinated to S atoms. The C–N stretching frequency $\nu(\text{C–N})$ appears at 2099 and 2121 cm^{-1} for structures **1** and **2**, respectively, both being higher than the one experimentally observed (2056 cm^{-1}). $\nu(\text{C–S})$ is found at 756 cm^{-1} in the first case, while in structure **2**, this value is lowered to 648 cm^{-1} . This feature clearly discards the existence of the S-bonded isomer because the experimental spectrum lacks any band in the region of 500–700 cm^{-1} . The $\delta(\text{NCS})$ bending mode is found at 465 and 438 cm^{-1} for structures **1** and **2**, respectively (484 cm^{-1} in the experimental spectrum). Finally, bands at 242 and 210 cm^{-1} are observed for the stretching modes Y–N and Y–S. Although this region of the spectrum was not recorded by the authors, both values are within the ranges observed in experimental studies.^{4a} In summary, for structure **1**, differences between predicted frequencies and those observed experimentally are below 5%, indicating that the N-coordinated isomer is the closest to the available experimental information. The measured and calculated values are in very good agreement with the measured and calculated values for the linkage isomers of pentachlorothiocyanatorhenato(IV) complexes.³⁹

Conclusions

The structure of the $[\text{Y}(\text{SCN})_6]^{3-}$ complex has been determined both in the solid state and in acetonitrile solution with EXAFS, IR, and NMR spectroscopies. The best reproduction of the EXAFS spectra was achieved for a symmetric octahedral complex coordinating through the N atom with $\angle\text{YNC}$ and $\angle\text{NCS}$ angles equal to 180° and with coordination distances at 2.36(1), 3.5(1), and 5.1(2) Å for Y–N, Y–C, and Y–S shells, respectively. This structure is compatible with IR and NMR experimental results. Single and multiple scattering contributions have been considered in the EXAFS analysis, with special relevance being the scattering paths that included strings of aligned atoms. No structural changes are induced by packing conditions or by solvent effects, as deduced from the comparison of the solid and solutions spectra, the only difference between both systems being the higher dynamic disorder of the solution. DFT calculations agree to a very good extent with the EXAFS results and confirm the IR bands ascription. Moreover, they explain the coordination through the N atom, since the N-coordinated complex is 115 kcal/mol more stable than the S-coordinated one, thus confirming the HSAB principle.

Acknowledgment. Thanks are due to the Photon Factory of the Institute of Material Structure Science (Project No. 95-G215) at KEK, Tsukuba, for beam time allocation and to Spanish DGICYT (Project No. PB95-549) for financial support. Dr. J. J. Rehr from Seattle University is acknowledged for the use of his FEFF program. Drs. L. J. Sánchez and E. Sánchez Marcos from Sevilla University are thanked for recording the NMR spectra and for helpful discussions. Dr. T. Miyanaga from Hiroaki University and Mr. S. Kawauchi from Osaka University are acknowledged for their assistance during the recording of the EXAFS spectra.

Supporting Information Available: Three tables containing input and output file parameters for a fit to the solid-state $[\text{Bu}_4\text{N}]_3[\text{Y}(\text{NCS})_6]$ spectrum, and two figures indicating the experimental and calculated EXAFS functions in acetonitrile solution and the magnitude and imaginary part of the Y–N phase-corrected Fourier transform EXAFS spectra (4 pages). Ordering information is given on any current masthead page.

References and Notes

- (1) Edelman, F. T. In *Comprehensive Organometallic Chemistry II*; Abel, E. W., Stone, F. A. G., Wilkinson, G., Eds.; Pergamon Press: Oxford, U.K., 1995; Vol. 4, p 11.
- (2) Cotton, S. In *Lanthanides and Actinides*; Adams, D. M., Green, M., Eds.; McMillan Physical Science Series; McMillan Education: London, U.K., 1991.
- (3) Forsters, D.; Goodgame, D. M. L. *J. Am. Chem. Soc.* **1965**, *87*, 268.
- (4) (a) Sabatini, A.; Bertini, I. *Inorg. Chem.* **1965**, *4*, 959. (b) Brown, T. M.; Knox, G. F. *J. Am. Chem. Soc.* **1967**, *89*, 5296.
- (5) (a) Kargol, J. A.; Creceley, R. W.; Burmeister, J. L. *Inorg. Chem.* **1979**, *18*, 2532. (b) Kidd, R. G.; Spinney, H. G. *J. Am. Chem. Soc.* **1981**, *103*, 4759. (c) Bailey, R. A.; Kozak, S. L.; Michelson, T. W.; Mills, W. L. *Coord. Chem. Rev.* **1971**, *6*, 407.
- (6) (a) Cotton, F. A.; Davison, A.; Ilsey, W. H.; Trop, H. S. *Inorg. Chem.* **1979**, *18*, 2719. (b) Trop, H. S.; Davison, A.; Jones, A. G.; Davis, M. A.; Szalda, D. J.; Lippard, S. J. *Inorg. Chem.* **1980**, *19*, 1105. (c) Knox, J. R.; Eriks, K. *Inorg. Chem.* **1968**, *7*, 84.
- (7) Ohtaki, H.; Radnai, T. *Chem. Rev.* **1993**, *93*, 1157.
- (8) (a) Persson, I.; Iverfelt, A.; Ahland, S. *Acta Chem. Scand. Ser. A* **1976**, *30*, 270. (b) Yamaguchi, T.; Yamamoto, K.; Ohtaki, H. *Bull. Chem. Soc. Jpn.* **1985**, *58*, 3235. (c) Ishiguro, S. I.; Ohtaki, H. *J. Coord. Chem.* **1987**, *15*, 237.
- (9) Stern, E. A. In *X-ray Absorption: Principles, Applications, Techniques of EXAFS, SEXAFS and XANES*; Koningsberger, D. C., Prins, R., Eds.; Wiley-Interscience: New York, 1988; p 3.
- (10) (a) Muñoz-Páez, A.; Sánchez Marcos, E. *J. Am. Chem. Soc.* **1992**, *114*, 6931. (b) Muñoz-Páez, A.; Pappalardo, R. R.; Sánchez Marcos, E. *J. Am. Chem. Soc.* **1995**, *117*, 11710. (c) Sakane, H.; Muñoz-Páez, A.; Díaz-Moreno, S.; Martínez, J. M.; Pappalardo, R. R.; Sánchez-Marcos, E. *J. Am. Chem. Soc.*, in press.
- (11) Díaz-Moreno, S.; Muñoz-Páez, A.; Martínez, J. M.; Pappalardo, R. R.; Sánchez Marcos, E. *J. Am. Chem. Soc.* **1996**, *118*, 12654.
- (12) (a) Miyanaga, T.; Sawa, Y.; Sakane, H.; Watanabe, I. *Physica B* **1995**, *208–209*, 393. (b) Tanida, H.; Sakane, H.; Watanabe, I. *J. Chem. Soc., Dalton Trans.* **1994**, 2321. (c) Sakane, H.; Watanabe, I.; Ono, K.; Ikeda, S.; Kaizaki, S.; Kushii, Y. *Inorg. Chim. Acta* **1990**, *178*, 67.
- (13) Ozutsumi, K.; Takamaku, T.; Ishiguro, S.; Ohtaki, H. *Bull. Chem. Soc. Jpn.* **1992**, *65*, 2104.
- (14) Martin, J. L.; Thompson, L. C.; Radonovich, L. J.; Glick, M. D. *J. Am. Chem. Soc.* **1968**, *90*, 4493.
- (15) Bailey, R. A.; Michelsen, T. W.; Mills, W. N. *J. Inorg. Nucl. Chem.* **1971**, *33*, 3206.
- (16) Dobado, J. A.; Ugglá, R.; Sundberg, M. R.; Molina, J. *Inorg. Chem.*, submitted.
- (17) Ziegler, T. *Chem. Rev.* **1991**, *91*, 651.
- (18) Estrin, D. A.; Hamra, O. Y.; Paglieri, L.; Slep, L.; Olabe, J. A. *Inorg. Chem.* **1996**, *35*, 6832.
- (19) Mire, L. W.; Wheeler, S. D.; Wagenseller, E.; Marynick, D. S. *Inorg. Chem.* **1998**, *37*, 3099.
- (20) Sánchez Marcos, E.; Gil, M.; Sánchez Marcos, A.; Martínez, J. M.; Muñoz-Páez, A. *Rev. Sci. Instrum.* **1994**, *65*, 2153.
- (21) Vaarkamp, M.; Linders, J. C.; Koningsberger, D. C. *Physica B* **1995**, *208–209*, 159.
- (22) Zabinsky, S. I.; Rehr, J. J.; Ankudinov, A.; Albers, R. C.; Eller, M. J. *Phys. Rev. B* **1995**, *52*, 2995.
- (23) Mustre de León, J.; Rehr, J. J.; Zabinsky, S. I.; Albers, R. C. *Phys. Rev. B* **1991**, *44*, 4146.
- (24) Frisch, M. J.; Trucks, G. W.; Schlegel, H. B.; Gill, P. M. W.; Johnson, B. G.; Robb, M. A.; Cheeseman, J. R.; Keith, T.; Petersson, G. A.; Montgomery, J. A.; Raghavachari, K.; Al-Laham, M. A.; Zakrzewski, V. G.; Ortiz, J. V.; Foresman, J. B.; Cioslowski, J.; Stefanov, B. B.; Nanayakkara, A.; Challacombe, M.; Peng, C. Y.; Ayala, P. Y.; Chen, W.; Wong, M. W.; Andres, J. L.; Replogle, E. S.; Gomperts, R.; Martin, R. L.; Fox, D. J.; Binkley, J. S.; Defrees, D. J.; Baker, J.; Stewart, J. P.; Head-Gordon, M.; Gonzalez, C.; Pople, J. A. *Gaussian 94*, revision E.2; Gaussian, Inc.: Pittsburgh, PA, 1995.
- (25) Dunning, T. H., Jr.; Hay, P. J. *Modern Theoretical Chemistry*; Plenum: New York, 1976.

- (26) (a) Hay, P. J.; Wadt, W. R. *J. Chem. Phys.* **1985**, 82, 270. (b) Wadt, W. R.; Hay, P. J. *J. Chem. Phys.* **1985**, 82, 284. (c) Hay, P. J.; Wadt, W. R. *J. Chem. Phys.* **1985**, 82, 299.
- (27) Becke, A. D. *J. Chem. Phys.* **1993**, 98, 5648.
- (28) Meehan, P. R.; Alyea, E. C.; Shakya, R. P.; Ferguson, G. *Polyhedron* **1998**, 17, 11.
- (29) Muñoz-Paez, A.; Ruiz-López, M. F. *J. Phys. Chem.* **1995**, 99, 16499.
- (30) Kuzmin, A.; Purans, J.; Parent, Ph. *Physica B* **1995**, 208–209, 45.
- (31) Gurman, S. J.; Binstead, N.; Ross, I. *J. Phys. C* **1984**, 17, 143.
- (32) Filipponi, A.; Di Cicco, A.; Natoli, C. R. *Phys. Rev. B* **1995**, 52, 15122.
- (33) O'Day, P. A.; Rehr, J. J.; Zabinsky, S. I.; Brown, G. E. *J. Am. Chem. Soc.* **1994**, 116, 2938.
- (34) Scott, M. J.; Zhang, H. H.; Lee, S. C.; Hedman, B.; Hodgson, K. O.; Holm, R. H. *J. Am. Chem. Soc.* **1995**, 117, 568.
- (35) Zhang, H. H.; Filipponi, A.; Di Cicco, A.; Scott, M. J.; Holm, R. H.; Hedman, B.; Hodgson, K. O. *J. Am. Chem. Soc.* **1997**, 119, 2470.
- (36) (a) Benafatto, M.; Natoli, C. R.; Bianconi, A.; García, J.; Marcelli, A.; Fanfoni, M.; Davoli, I. *Phys. Rev. B* **1986**, 34, 5774 (b) Filipponi, A.; D'Angelo, P.; Viorel Pavel, N.; Di Cicco, A. *Chem. Phys. Lett.* **1994**, 225, 150.
- (37) D'Angelo, P.; Di Nola, A.; Giglio, E.; Mangani, M.; Pavel, N. V. *J. Phys. Chem.* **1995**, 99, 5471.
- (38) Parr, R. G.; Yang, W. *Density functional theory of atoms and molecules*; Oxford University Press: Oxford, 1989.
- (39) Semrau, M.; Preetz, W.; Holmoya, L. *Z. Anorg. Allg. Chem.* **1997**, 623, 179.
- (40) (a) Binkley, J. S.; Pople, J. A.; Hehre, W. *J. Am. Chem. Soc.* **1980**, 102, 939. (b) Gordon, M. S.; Binkley, J. S.; Pople, J. A.; Pietro, W. J.; Hehre, W. *J. Am. Chem. Soc.* **1982**, 104, 2797. (c) Pietro, W. J.; Francl, M. M.; Hehre, W. J.; Defrees, D. J.; Pople, J. A.; Binkley, J. S. *J. Am. Chem. Soc.* **1982**, 104, 5039.